

**NO₂ and HCHO
photolysis
frequencies**

C. Topaloglou et al.

NO₂ and HCHO photolysis frequencies from irradiance measurements in Thessaloniki, Greece

C. Topaloglou¹, S. Kazadzis¹, A. F. Bais¹, M. Blumthaler², B. Schallhart², and
D. Balis¹

¹Laboratory of Atmospheric Physics, Aristotle University of Thessaloniki, Greece

²Division for Biomedical Physics, Innsbruck Medical University, Austria

Received: 9 February 2005 – Accepted: 8 March 2005 – Published: 15 March 2005

Correspondence to: C. Topaloglou (ctopa@skiathos.physics.auth.gr)

© 2005 Author(s). This work is licensed under a Creative Commons License.

Title Page

Abstract

Introduction

Conclusions

References

Tables

Figures

◀

▶

◀

▶

Back

Close

Full Screen / Esc

Print Version

Interactive Discussion

EGU

Abstract

An empirical approach for the retrieval of nitrogen dioxide (NO_2) and formaldehyde (HCHO) photolysis frequencies from measurements of global irradiance is presented in this work. Four months of synchronous measurements of actinic flux and global irradiance performed in Thessaloniki, Greece by a Bentham spectroradiometer were used to extract polynomials for the conversion of global irradiance to photolysis frequencies [$J(\text{NO}_2)$ and $J(\text{HCHO})$]. The comparison of these photolysis frequency values to the corresponding values calculated by spectral actinic flux measurements, showed a ratio very close to unity for all J 's with a standard deviation of 6% for $J(\text{NO}_2)$ and 3% for $J(\text{HCHO})$. Additional sets of polynomials were also extracted to allow determination of $J(\text{NO}_2)$ by spectroradiometers with lower upper wavelength limits such as single and double Brewer spectroradiometers within acceptable uncertainty (corresponding ratio was 1 and standard deviation was 6% for double and 10% for single Brewers). The validity of the method under different atmospheric conditions was also examined by applying the polynomials to another set of actinic flux and global irradiance measurements performed in May 2004, in Buchhofen, Germany. In this case, comparing J values extracted from the polynomials to those calculated from actinic flux, showed equivalent results, demonstrating that the method can also be applied to other measurement sites.

1. Introduction

The photodissociation of trace gases in the atmosphere is a process of great importance for atmospheric chemistry. Solar ultraviolet radiation drives the photolysis of several species, such as NO_2 and HCHO, contributing to their decomposition and removal from the atmosphere as well as the formation of highly reactive radicals. Photodissociation is the dominant loss process for NO_2 (Eq. 1), producing $\text{O}(^3\text{P})$ atoms which enable tropospheric ozone formation (Eq. 2). However, NO produced from reaction

NO_2 and HCHO photolysis frequencies

C. Topaloglou et al.

Title Page

Abstract

Introduction

Conclusions

References

Tables

Figures

◀

▶

◀

▶

Back

Close

Full Screen / Esc

Print Version

Interactive Discussion

NO₂ and HCHO photolysis frequencies

C. Topaloglou et al.

Title Page

Abstract

Introduction

Conclusions

References

Tables

Figures

◀

▶

◀

▶

Back

Close

Full Screen / Esc

Print Version

Interactive Discussion

EGU

(1) is oxidized back to NO₂, consuming ozone in this case (Eq. 3), see e.g. He and Charmichael, (1999):



The NO₂ photodissociation process itself as well as the NO-NO₂ equilibrium in the NO_x, (also influenced by NO₂ photolysis) are closely related to the radical cycles of OH and HO₂ (Kraus et al., 2000) and are an important parameter for tropospheric ozone concentrations.

10 Formaldehyde is one of the most important and abundant organic carbonyl compounds in the atmosphere, observed in both polluted urban and rural environments. It is mainly produced from fossil fuel combustion and is also a secondary product of photochemical oxidation of methane and other hydrocarbons (Meller and Moortgat, 2000). The processes (Eq. 4) and (Eq. 5) presented below achieve the photolysis of
15 formaldehyde:



The photolysis of formaldehyde plays a significant role in the formation of photochemical smog, through the generation of HO₂ radicals which participate in O₃c catalytic production (Smith et al., 2002). Both H and HCO produced from Eq. (4), yield
20 HO₂ radicals as shown in chemical reactions presented in Eqs. (6) and (7):



**NO₂ and HCHO
photolysis
frequencies**

C. Topaloglou et al.

It is therefore of considerable importance for atmospheric chemistry to accurately determine the photolysis rates of key atmospheric compounds such as NO₂ and HCHO. In the past, chemical actinometers and filter radiometers have been used to measure $J(\text{NO}_2)$ (e.g. Dickerson et al., 1982; Shetter et al., 1992; Lantz et al., 1996; Balis et al., 2002, Shetter et al., 2003). Similar measurements for other photolysis rates such as $J(\text{HCHO})$, were not as common as in the case of NO₂ or O₃, due to considerable requirements concerning the development and maintenance of these instruments, so those rates were either estimated or modeled (Kraus and Hofzumahaus, 1998). In the last decade, spectroradiometric measurements of actinic flux have developed enabling the determination of photolysis rates for several atmospheric species as the integral:

$$J = \int_{\lambda_1}^{\lambda_2} F(\lambda) \sigma(\lambda, T) \phi(\lambda, T) d\lambda, \quad (8)$$

where $\sigma(\lambda, T)$ is the absorption cross section of the molecule, $\phi(\lambda, T)$ the photodissociation quantum yield, (both dependant on wavelength and temperature) and $F(\lambda)$ the spectral actinic flux. Photolysis rate determination by means of spectroradiometry has been reported in the last decade for both NO₂ (McElroy et al., 1995; Kraus and Hofzumahaus, 1998; Shetter and Müller, 1999; Edwards and Monks, 2003, Shetter et al., 2003) and formaldehyde (Kraus and Hofzumahaus, 1998; Shetter and Müller, 1999). However, since actinic flux measurements are not trivial, several approaches have been developed in order to enable the use of global irradiance instead of actinic flux for photolysis rate determination. Previous work includes the transformation of global irradiance to actinic flux (Cotté et al., 1997; Kazadzis et al., 2000; Webb et al., 2002; Kylling et al., 2003; Schallhart et al., 2004) which can then be used for photolysis rate determination, as well as empirical methods to derive photolysis rates directly from global irradiance measurements (McKenzie et al., 2002; Kazadzis et al., 2004; Seroji et al., 2004).

This work presents an empirical method to determine photolysis rate values for NO₂ and HCHO from measurements of global irradiance from a Bentham spectroradiome-

[Title Page](#)[Abstract](#)[Introduction](#)[Conclusions](#)[References](#)[Tables](#)[Figures](#)[◀](#)[▶](#)[◀](#)[▶](#)[Back](#)[Close](#)[Full Screen / Esc](#)[Print Version](#)[Interactive Discussion](#)

**NO₂ and HCHO
photolysis
frequencies**

C. Topaloglou et al.

ter. First, the variability of actinic flux to global ratio as a function of solar zenith angle (sza) is discussed. Then the empirical method is presented in detail and is implemented on global irradiance data. The photolysis frequency values produced by the method are compared to corresponding values derived from measured actinic flux.

5 Additional polynomials are extracted using global irradiance at wavelengths suitable for the use of Brewer spectroradiometer measurements. The results comparing J values derived from this method to those calculated from actinic flux are presented for all cases. Finally, the performance of the method applied to measurements from a different measurement site is examined, showing satisfactory results.

10 2. Data and instrumentation

The UV global irradiance and actinic flux spectra used in this study to extract the polynomials for the empirical method were measured by a Bentham DTM 300 (Division for Biomedical Physics, Innsbruck Medical University), installed at the roof of the Physics Department in Thessaloniki, at the Laboratory of Atmospheric Physics (LAP) from March to July 2003. The instrument performed synchronous measurements of actinic flux and global irradiance from 290 to 500 nm, in the framework of the INSPECTRO project (Influence of clouds on the Spectral actinic flux in the lower Troposphere, <http://imk-ifu.fzk.de/inspectro/index.html>). In addition, a double-monochromator Brewer MKIII spectroradiometer provided UV spectral global irradiance measurements in the range of 287–366 nm. Finally, total irradiance from a Kipp and Zonnen CM21 pyranometer was used to enable cloud flagging of the spectra. During the INPSECTRO project the Bentham instrument also measured actinic and global irradiance at Buchhofen, Germany, in May 2004.

Detailed information on both the instrument characteristics and calibration details can be found in Kazadzis et al. (2004). A summary of the information on the instruments, the locations and the periods of the measurements that are used in both methods presented in this paper are shown in Table 1.

Title Page

Abstract

Introduction

Conclusions

References

Tables

Figures

◀

▶

◀

▶

Back

Close

Full Screen / Esc

Print Version

Interactive Discussion

EGU

3. Empirical method for $J(\text{NO}_2)$ retrieval

3.1. Variability of the ratio of actinic flux to global irradiance

The basic idea of this method is the determination of $J(\text{NO}_2)$ as a function of solar zenith angle, by the use of global irradiance and empirical relationships, instead of the direct way using actinic flux and Eq. (8). For all $J(\text{NO}_2)$ calculations in this work, the absorption cross-section and quantum yield of DeMore et al. (1997) were used at the temperature of 298°K. Examining the wavelength dependence of the $J(\text{NO}_2)$ rate using the molecule functions mentioned above, it appears that the spectral weighting of the solar radiation spectrum by this process is largest in the region between 375 and 400 nm. The relative contribution of each wavelength to the $J(\text{NO}_2)$ calculation for 12 May 2003, $\text{sza}=24^\circ$, is shown in Fig. 1. The contribution of the 375–400 region is around 40%. As a result, the integral of global irradiance in this spectral region was selected as the global irradiance quantity to be used for the $J(\text{NO}_2)$ determination.

Since the method aims to use global irradiance instead of actinic flux, the variability of downwelling actinic flux to global irradiance is discussed briefly. The ratio actinic flux/global irradiance as a function of solar zenith angle for wavelength of 390 nm is shown in Fig. 2. All ratio values are above unity since actinic flux is a quantity measured by a spherical detector while global irradiance by a flat one. Lowest values of the ratio (around 1.35) represent small solar zenith angles and low aerosol load, where the highest values (around 2.6) appear around 75 degrees of sza and refer to cloudless conditions with small aerosol optical depth (AOD) as well. The overall shape of the ratio distribution is a result of the diminished contribution of the direct component to the global irradiance as solar zenith angle increases. Consequently, high values of this ratio around 75° , characterize this spectral region because of the more significant contribution of the direct component in comparison to the diffuse in these wavelengths. Since overcast spectra give an almost constant value of actinic/global ratio for all sza , around 1.75, it is apparent that the larger variability of this ratio is to be found at solar zenith angles around $70\text{--}75^\circ$. The variability due to different cloud cover conditions as

Title Page

Abstract

Introduction

Conclusions

References

Tables

Figures

◀

▶

◀

▶

Back

Close

Full Screen / Esc

Print Version

Interactive Discussion

well as various AOD loads, account for the vertical distribution of the data in Fig. 2, for a single solar zenith angle.

3.2. Description of the method

$J(\text{NO}_2)$ values were determined by Eq. (8) using spectral actinic flux measurements and the (375–400 nm) global irradiance integral ($E_{375-400}$) calculated from simultaneous global irradiance spectra. The two quantities are shown in Fig. 3. As it can be observed, $J(\text{NO}_2)$ is closely correlated to $E_{375-400}$ and its variability for a given irradiance value is rather small.

The dataset was divided into groups of 5° sza and 2nd degree polynomials were calculated from least squares fits between the $J(\text{NO}_2)$ and ($E_{375-400}$). The polynomial coefficients are shown in Table 3. $J(\text{NO}_2)$ values were then recalculated using these polynomials (J_{calc}) and were compared to $J(\text{NO}_2)$ values from actinic flux spectra using Eq.8. Their average ratio $\frac{J_{\text{calc}}}{J(\text{NO}_2)}$ was 1.001 ± 0.062 (1σ) including all solar zenith angles, cloud cover and aerosol load conditions (Fig. 4).

The variability of the ratio shown in Fig. 4 is related to the representativeness of the polynomials. The scatter for a constant sza is smaller in the region of 40-50 degrees, ($2\sigma=0.12$), is consistent with the limited variation of the actinic to global ratio as demonstrated in Fig. 2. This means that the polynomials can more accurately reproduce the $J(\text{NO}_2)$ values from the global irradiance value for these solar zenith angles. On the other hand, the increase of the ratio variability for solar zenith angles larger than 55 degrees reflects the greater variability of the actinic flux to global irradiance ratio at these angles ($2\sigma=0.44$ for $70-75^\circ$ sza) also shown in Fig. 2.

In order to decrease the method uncertainty, a parameterization with cloud conditions was examined. The spectra used in this work were characterized according to cloud cover from a methodology proposed by Vasaras et al. (2000). Pyranometer data were used to determine the variability of the radiation field due to clouds for each scan, which was flagged as 0 (sun not occluded, stable radiation field), 1 (sun oc-

Title Page

Abstract

Introduction

Conclusions

References

Tables

Figures

◀

▶

◀

▶

Back

Close

Full Screen / Esc

Print Version

Interactive Discussion

**NO₂ and HCHO
photolysis
frequencies**

C. Topaloglou et al.

cluded, stable radiation field), or 2 (broken clouds, unstable radiation field). For scans flagged as 0 and 2, data were again divided into groups of 5° sza and new polynomials were extracted for each group to produce $J(\text{NO}_2)$ from $E_{375-400}$. For scans flagged as 1, $J(\text{NO}_2)$ and $E_{375-400}$ were very successfully correlated by a linear approximation, where $R^2=0.99$, so this linear expression was used in this case for all solar zenith angles.

The application of the new -cloud dependent- polynomials on the Bentham data, produced an overall mean value of 0.999 for the $\frac{J_{\text{calc}}}{J(\text{NO}_2)}$ ratio, with a standard deviation of 0.06. It is apparent that no significant change is evident for the entire data set.

Small differences between the $\frac{J_{\text{calc}}}{J(\text{NO}_2)}$ ratio from the original method to the one with cloud flagging have been observed, when examining each set of data (Flag 0, 1 and 2) individually, as seen in Table 2. The absolute value of $J(\text{NO}_2)$ derived from Flag 1 spectra is improved by approx. 1.5%, using the cloud dependent polynomials. The remaining flag cases have significantly smaller deviations.

3.3. Alternative polynomials for Brewer spectroradiometers

To enable the use of the method described above by spectroradiometers that do not reach 400 nm, such as double or single Brewer monochromators (upper wavelength limit 365 nm and 325 nm, respectively), similar approaches were developed by using global irradiance at 360 nm (E_{360}) for double Brewer spectrometer and 325 nm (E_{325}) for single Brewer spectrometer, as an independent variable instead of $E_{375-400}$. A new set of polynomials was extracted for each case, using once more Bentham simultaneous actinic flux and global irradiance measurements. The corresponding ratios of $\frac{J_{\text{calc}}}{J(\text{NO}_2)}$ for these two cases are shown in Fig. 5.

The use of global irradiance at 360 nm as the independent variable does not significantly change the results of the application of this method. The ratio of $\frac{J_{\text{calc}}}{J(\text{NO}_2)}$ is 0.999 with as standard deviation of 0.067. In the case of 325 nm, this ratio continues to be very close to unity, namely 1.003, however the standard deviation increases

[Title Page](#)[Abstract](#)[Introduction](#)[Conclusions](#)[References](#)[Tables](#)[Figures](#)[◀](#)[▶](#)[◀](#)[▶](#)[Back](#)[Close](#)[Full Screen / Esc](#)[Print Version](#)[Interactive Discussion](#)

EGU

**NO₂ and HCHO
photolysis
frequencies**

C. Topaloglou et al.

Title Page

Abstract

Introduction

Conclusions

References

Tables

Figures

◀

▶

◀

▶

Back

Close

Full Screen / Esc

Print Version

Interactive Discussion

EGU

considerably, especially as mentioned before for large solar zenith angles and reaches 0.107. This means that the average values of $J(\text{NO}_2)$ can still be reproduced, but greater uncertainty is introduced by the fact that in the course of the spectral scan the 325 nm wavelength is measured several minutes before the 375–400 nm region, which is highly representative of the $J(\text{NO}_2)$ value. Rapid changes of the radiation field caused by moving clouds in front of the sun, could result to a non representative irradiance value at 325 nm, for this photolysis frequency calculation.

To test the validity of this method, global irradiance spectra from a double Brewer MKIII spectrometer working in LAP were used to produce $J(\text{NO}_2)$ values. The data were corrected for calibration standard differences between the two instruments and for possible wavelength shifts, using SHICRIVM (Slaper et al., 1995), an algorithm that also deconvolutes the measured spectra to a standard slit with 1 nm FWHM (the methodology is discussed in Kazadzis et al., 2004). The photolysis frequencies produced by Brewer irradiance from global spectra and the polynomials, J_{BREWER} , were then compared to $J(\text{NO}_2)$ values from Bentham's actinic flux spectra, for measurements that deviated from each other less than 5 min. The results for the use of both (single and double) Brewer cases are presented in Fig. 6.

The results showed a mean ratio of 1.004 ± 0.137 for the use of E_{360} and 1.019 ± 0.163 for the use of E_{325} as independent parameters. The same pattern with the increase of the ratio variability for large solar zenith angles also appears in these results. The total uncertainty is greater in this case, because of additional factors affecting the quality of the results, such as measuring differences between the instruments. Another reason for the dispersion of the ratios around unity could be the time difference (the order of a few minutes) between the Brewer and Bentham scans, a potentially significant factor leading to large deviations in cases with variable cloud cover.

3.4. Implementation of the method on data from different locations

Finally, in order to investigate the extent to which the method is valid for other measurement sites, global irradiance and actinic flux data from the Bentham instrument

**NO₂ and HCHO
photolysis
frequencies**

C. Topaloglou et al.

Title Page

Abstract

Introduction

Conclusions

References

Tables

Figures

◀

▶

◀

▶

Back

Close

Full Screen / Esc

Print Version

Interactive Discussion

EGU

from a field campaign of INSPECTRO in May 2004 were used. The Bentham performed measurements in Buchhofen, Germany (48.7° N, 12.9° E, 340 m) from 13–22 May, 2004. $J(\text{NO}_2)$ values were calculated from the $E_{375-400}$ integral and the polynomials retrieved from Thessaloniki's dataset. The results were then compared to $J(\text{NO}_2)$ directly from actinic flux and Eq. (8). The results are shown in Fig. 7. The mean $\frac{J_{\text{calc}}}{J(\text{NO}_2)}$ ratio for $\text{sza} < 85^\circ$ is 1.001 and the standard deviation is 0.063, showing that the polynomials seem to reproduce the $J(\text{NO}_2)$ values satisfactorily. The observation site in Buchhofen is rural, therefore the amount and type of aerosols is expected to be different compared to the measurements in Thessaloniki. The atmospheric pattern for this period was dominated by partly cloudy and overcast sky conditions, with occasional clear sky intervals. The application of the method to this data set showed generally good agreement among measured and calculated photolysis frequencies.

4. Empirical method for J(HCHO) retrieval

A similar empirical method could be used for calculating HCHO photolysis rates. However, since the spectral region of interest of the HCHO photolysis is between 280 and 360 nm, special consideration has to be given to the fact that radiation in this spectral region is affected by ozone in the atmosphere. For this reason, instead of directly associating the HCHO photolysis rates to global irradiance, the ratio J/J_{pseudo} is used where J is the photolysis frequency value calculated from Eq. (8) using actinic flux and J_{pseudo} is the corresponding value when global irradiance is integrated instead of actinic flux. This ratio is associated with global irradiance at 325 nm. Both the ratio and the irradiance quantity are independent of ozone, so the method is to be used for all total ozone column conditions. 3rd degree polynomials are extracted for 5° sza groups. To calculate the $J(\text{HCHO})$, the global irradiance at 325 nm is used together with the extracted polynomials and finally a J/J_{pseudo} ratio is calculated. The ratio is then multiplied with J_{pseudo} integrated from spectral global irradiance measurements, to produce the $J(\text{HCHO})$ value. The molecular data for $J(\text{HCHO})$ determination used

in this work are the cross section from Meller et Moortgat (2000) and the quantum yield from DeMore et al. (1997). The extracted polynomials for both chemical reactions are presented in Tables 4 and 5.

The method was applied to the measurements performed in Thessaloniki from April to July 2003, to produce $J(\text{HCHO})$ which were then compared to those calculated from actinic flux. The results are shown in Fig. 8:

The ratio $\frac{J_{\text{calc}}}{J(\text{HCHO})}$ is practically unity and the standard deviation for both chemical reactions is found around 3%. The decrease in the standard deviation value compared to that of the $J(\text{NO}_2)$ determination, derives from the fact that the variation of the actinic flux to global irradiance ratio is considerably smaller in the wavelength region of the formaldehyde photolysis, especially for larger solar zenith angles.

When applying this method to Brewer global irradiance data in order to produce $J(\text{HCHO})$ values, taking into consideration all factors already mentioned in the previous paragraph, the mean value of $\frac{J_{\text{BREWER}}}{J(\text{HCHO})}$ equals 0.987 and a standard deviation of 0.097 for chemical reaction (R1) and 0.989 ± 0.093 for reaction (R2). Finally, when applying the method to the Bentham data in Buchhofen from May 2004, the ratio of the calculated $J(\text{HCHO})$ to those determined from actinic flux is found to be 0.989 ± 0.038 for (R1) and 0.996 ± 0.042 for (R2) for $\text{sza} < 85^\circ$. This small deviation of the mean ratio from unity is a result of the implementation of the polynomials extracted in Thessaloniki, an urban site with several clear sky days during the year, to data from a rural and mostly cloudy (at the time of the measurements) site. It should also be noted that all σ values presented in this study are related to the uncertainty of the method itself and that the total uncertainty of the J values also includes cross section and quantum yield uncertainty as well as measuring uncertainties.

**NO₂ and HCHO
photolysis
frequencies**C. Topaloglou et al.

[Title Page](#)[Abstract](#)[Introduction](#)[Conclusions](#)[References](#)[Tables](#)[Figures](#)[◀](#)[▶](#)[◀](#)[▶](#)[Back](#)[Close](#)[Full Screen / Esc](#)[Print Version](#)[Interactive Discussion](#)

5. Conclusions

Two approaches of an empirical method for calculating $J(\text{NO}_2)$ and $J(\text{HCHO})$ are presented, based on spectral measurements of global irradiance and the use of polynomials, as a function of solar zenith angle. The ratio of J values derived from these methods to those calculated directly by actinic flux spectra is 1.001 with a standard deviation of around 6% for $J(\text{NO}_2)$, and for $J(\text{HCHO})$ 1.001 ± 0.03 for chemical reaction (R1) and 1.001 ± 0.03 for chemical reaction (R2), showing that nitrogen dioxide and formaldehyde photolysis frequencies can satisfactorily be reproduced by this method within acceptable uncertainty.

Alternative polynomials were extracted to enable the use of this method by Brewer spectroradiometers (double and single) and the ratio of photolysis rates from a Brewer spectroradiometer to those retrieved from actinic flux measurements from a Bentham spectroradiometer show a ratio of $\frac{J_{\text{Brewer}}}{J(\text{NO}_2)}$ equal to 1.004 ± 0.137 using 360 nm, 1.019 ± 0.163 using 325 nm, and for HCHO the ratio $\frac{J_{\text{Brewer}}}{J(\text{HCHO})}$ is 0.989 ± 0.093 for reaction (R1) and 0.987 ± 0.097 for reaction (R2), respectively. The level of agreement for $J(\text{HCHO})$ is similar to that of the global irradiance spectra measured by the two instruments for that spectral region.

Finally the method was applied also to measurements of the Bentham spectroradiometer, performed in Buchhofen, Germany, in May 2004 in order to examine whether it could be implemented to data from another measuring site. The results from comparing the rates calculated by these methods to those determined from Bentham's actinic flux spectra for $\text{sza} < 85^\circ$, show a ratio of 1.001 ± 0.063 for $J(\text{NO}_2)$ and for $J(\text{HCHO})$, 0.989 ± 0.038 reaction (R1) and 0.996 ± 0.042 for reaction (R2), demonstrating that the method can be applied to other measurement sites as well.

In the absence of routine actinic flux measurements due to the special configured optics required, the development of alternative methods to retrieve photolysis frequency values for NO_2 and HCHO can be very useful for atmospheric chemistry studies, since photolysis rates are an important input parameter for tropospheric chemistry models.

Title Page

Abstract

Introduction

Conclusions

References

Tables

Figures

◀

▶

◀

▶

Back

Close

Full Screen / Esc

Print Version

Interactive Discussion

**NO₂ and HCHO
photolysis
frequencies**

C. Topaloglou et al.

Ultraviolet (UV) global irradiance measurements are very common in monitoring stations worldwide and a global network has developed in the last 20 years, providing a long history of quality assured irradiance measurements. Therefore, the retrieval of photolysis rate values from global irradiance measurements allows the reproduction of extensive time series of photolysis rates for nitrogen dioxide and formaldehyde, within reasonable uncertainty.

Acknowledgements. Part of the work was conducted in the framework of the INSPECTRO EVK2-2001-00135 project, funded by the European Commission.

References

- Balis, D. S., Zerefos, C. S., Kourtidis, K., Bais, A. F., Hofzumahaus, A., Kraus, A., Schmitt, R., Blumthaler, M., and Gobbi, G. P.: Measurements and modeling of photolysis rates during the Photochemical Activity and Ultraviolet Radiation (PAUR) II campaign, *J. Geophys. Res.*, 107, D0, 8138–8149, 2002.
- Cotté, H., Devaux, C., and Carlier, P.: Transformation of irradiance measurements into spectral actinic flux for photolysis rates determination, *J. Atmos. Chem.*, 26, 1–28, 1997.
- De More, W., Sander, S., Golden, D., Hampson, R., Kurylo, M., Howard, C., Ravishankara, A., Kolb, C., and Molina, M.: Chemical kinetics and photochemical data for use in stratospheric modeling, *JPL Publ.*, 97-4, 1997.
- Dickerson, R. R., Stedman, D. H., and Delany, A. C.: Direct measurements of ozone and nitrogen dioxide photolysis rates in the troposphere, *J. Geophys. Res.*, 87, 4933–4946, 1982.
- Edwards, G. D. and Monks, P. S.: Performance of a single-monochromator diode array spectroradiometer for the determination of actinic flux and atmospheric photolysis frequencies, *J. Geophys. Res.*, 108, D16, 8546–8558, 2003.
- He, S. and Charnichael, G. R.: Sensitivity of photolysis rates and ozone production in the troposphere to aerosol properties, *J. Geophys. Res.*, 104, D21, 26 307–36 324, 1999.
- Kazadzis, S., Bais, A. F., Balis, D., Zerefos, C. S., and Blumthaler, M.: Retrieval of down-welling UV actinic flux density spectra from spectral measurements of global and direct solar UV irradiance, *J. Geophys. Res.*, 105, 4857–4864, 2000.

Title Page

Abstract

Introduction

Conclusions

References

Tables

Figures

◀

▶

◀

▶

Back

Close

Full Screen / Esc

Print Version

Interactive Discussion

EGU

**NO₂ and HCHO
photolysis
frequencies**

C. Topaloglou et al.

Title Page

Abstract

Introduction

Conclusions

References

Tables

Figures

◀

▶

◀

▶

Back

Close

Full Screen / Esc

Print Version

Interactive Discussion

EGU

Kazadzis, S., Topaloglou, C., Bais, A. F., Blumthaler, M., Balis, D., Kazantzidis, A., and Schallhart, B.: Actinic flux and O¹D photolysis frequencies retrieved from spectral of irradiance at Thessaloniki, Greece, *Atmos. Chem. Phys.*, 4, 2215–2226, 2004,

[SRef-ID: 1680-7324/acp/2004-4-2215.](#)

5 Kraus, A. and Hofzumahaus, A.: Field measurements of atmospheric photolysis frequencies for O₃, NO₂, HCHO, CH₃CHO, H₂O₂ and HONO by UV spectroradiometry, *J. Atm. Chem.*, 31, 161–180, 1998.

Kylling, A., Webb, A. R., Bais, A. F., Blumthaler, M., Schmitt, R., Thiel, S., Kazantzidis, A., Kift, R., Misslebeck, M., Schallhart, B., Schreder, J., Topaloglou, C., Kazadzis, S., and Rimmer, J.: Actinic flux determination from measurements of irradiance, *J. Geophys. Res.*, 108, D16, 4506–4515, 2003.

10 Lantz, K. O., Shetter, R. E., Cantrell, C. A., Flocke, S. J., Calvert, J. G., and Madronich, S.: Theoretical, actinometric and radiometric determinations of the photolysis rate coefficient of NO₂ during the Manua Loa Observatory Photochemistry Experiment 2., *J. Geophys. Res.*, 101, 14 613–14 629, 1996.

15 McElroy, C. T., Midwinter, C., Barton, D. V., and Hall, R. B.: A comparison of J-values from the composition and photodissociative flux measurements with model calculations, *Geophys. Res. Lett.*, 22, 11, 1365–1368, 1995.

20 McKenzie, R. L., Johnston, P. V., Hofzumahaus, A., Kraus, A., Madronich, S., Cantrell, C., Calvert, J., and Shetter, R.: Relationship between photolysis frequencies derived from spectroscopic measurements of actinic fluxes and irradiances during the IPMMI campaign, *J. Geophys. Res.*, 107, D5, 4042–4057, 2002.

Meller, R. and Moortgat G. K.: Temperature dependence of the absorption cross sections of formaldehyde between 223 and 323 K in the wavelength range 225–375 nm, *J. Geophys. Res.*, 105, D6, 7089–7101, 2000.

25 Schallhart, B., Huber M., and Blumthaler M.: Semi-empirical method for the conversion of spectral UV global irradiance data into actinic flux, *Atm. Env.*, 38, 4341–4346, 2004.

Seraji, A. R., Webb, A. R., and Coe, H.: Derivation and validation of photolysis rates of O₃, NO₂ and CH₂O from a GUV-541 radiometer, *J. Geophys. Res.*, 109, D21307, 2004.

30 Shetter, R. E., McDaniel, A. H., Cantrell, C. A., Madronich, S., and Calvert, J. G.: Actinometer and Eppley radiometer measurements of the NO₂ photolysis rate during the Manua Loa Observatory Photochemistry Experiment, *J. Geophys. Res.*, 97, 10 349–10 359, 1992.

Shetter, R. E. and Müller, M.: Photolysis frequency measurements using actinic flux spec-

troradiometry during the PEM-Tropics mission: Instrument description and some results, *J. Geophys. Res.*, 104, 5647–5661, 1999.

Shetter, R. E. Junkermann, W., Swartz, W. H., Frost G. J., Crawford, J. H., Lefer, B. L., Barrick, J. D., Hall, S. R., Hofzumahaus, A., Bais, A., Calvert, J. G., Cantrell, C. A., Madronich, S., Müller, M., Kraus, A., Monks, P. S., Edwards, G. D., McKenzie, R., Johnston, P., Schmitt, R., Griffioen, E., Krol, M., Kylling, A., Dickerson, R. R., Lloyd, S. L., Martin, T., Gardiner, B., Mayer, B., Pfister, G., Röth, E. P. Koepke, P., Ruggaber, A., Schwander, H., and Van Weele M.: Photolysis frequency of NO₂: Measurement and modeling during the International Photolysis Frequency Measurement and Modeling Intercomparison (IPMMI), *J. Geophys. Res.*, 108, D16, 8544–8558, 2003.

Smith, G. D., Molina, L. T., and Molina, M. J.: Measurement of radical quantum yields from formaldehyde photolysis between 269 and 339 nm, *J. Phys. Chem.*, 106, 1233–1240, 2002.

Vasaras, A., Bais, A. F., Feister, U., and Zerefos, C. S.: Comparison of two methods for cloud flagging of spectral UV measurements, *Atmos. Res.*, 57/1, 31–42, 2001.

Webb, A. R., Kift, R., Thiel, S., and Blumthaler, M.: An empirical method for the conversion of spectral UV irradiance measurements to actinic flux data, *Atmos. Environ.*, 36, 4044–4397, 2002.

Wiegand, A. N. and Bofinger N. D.: Review of empirical methods for the calculation of the diurnal NO₂ photolysis rate coefficient, *Atmos. Environ.*, 34, 99–108, 2000.

**NO₂ and HCHO
photolysis
frequencies**

C. Topaloglou et al.

Title Page

Abstract

Introduction

Conclusions

References

Tables

Figures

◀

▶

◀

▶

Back

Close

Full Screen / Esc

Print Version

Interactive Discussion

NO₂ and HCHO photolysis frequencies

C. Topaloglou et al.

Table 1. Description of instruments details, location and periods of measurements.

Instrument	Measurement quantity	Location	Period
Brewer MKII spectroradiometer	Global irradiance 287–366 nm	Thessaloniki, Greece	2003
Pyranometer	Total irradiance (305–800 nm)	Thessaloniki, Greece	2003
Bentham DTM300	Actinic flux 290–550 nm	Thessaloniki, Greece	March–July 2003
Spectroradiometer	Global irradiance 290–550 nm	Buchhofen, Germany	13–22 May 2004

[Title Page](#)
[Abstract](#)
[Introduction](#)
[Conclusions](#)
[References](#)
[Tables](#)
[Figures](#)
[Back](#)
[Close](#)
[Full Screen / Esc](#)
[Print Version](#)
[Interactive Discussion](#)

NO₂ and HCHO photolysis frequencies

C. Topaloglou et al.

Table 2. Mean values of $\frac{J_{\text{calc}}}{J(\text{NO}_2)}$ ratio for each group of spectra, using the original polynomials and the cloud dependent polynomials.

Type of spectra	Polynomials without cloud flagging Mean ratio $\pm\sigma$	Polynomials with cloud flagging Mean ratio $\pm\sigma$
Flag 0	0.996 \pm 0.038	1.001 \pm 0.037
Flag 1	1.029 \pm 0.08	1.012 \pm 0.056
Flag 2	1.005 \pm 0.072	1.005 \pm 0.069

[Title Page](#)
[Abstract](#)
[Introduction](#)
[Conclusions](#)
[References](#)
[Tables](#)
[Figures](#)
[◀](#)
[▶](#)
[◀](#)
[▶](#)
[Back](#)
[Close](#)
[Full Screen / Esc](#)
[Print Version](#)
[Interactive Discussion](#)

EGU

NO₂ and HCHO photolysis frequencies

C. Topaloglou et al.

Table 3. Polynomial coefficients for the calculation of $J(\text{NO}_2)=f(E_{375-400\text{nm}})$. C_i represents the i degree coefficient.

Solar zenith angle (°)	C_2 ($\times 10^{-6}$)	C_1 ($\times 10^{-4}$)	C_0 ($\times 10^{-5}$)
15–20	–9.09	5.53	9.246
20–25	–9.64	5.79	–14.548
25–30	–7.95	5.37	4.370
30–35	–8.34	5.62	–19.156
35–40	–7.28	5.47	–10.541
40–45	–6.68	5.49	–14.003
45–50	–3.97	5.25	–10.263
50–55	0.012	5.02	–9.151
55–60	3.22	5.02	–10.216
60–65	6.32	5.11	–12.000
65–70	9.31	5.22	–11.906
70–75	24.2	4.66	–4.895
75–80	53.5	3.79	3.422
80–85	40.8	4.35	0.578
85–90	43.6	4.35	0.374

[Title Page](#)
[Abstract](#)
[Introduction](#)
[Conclusions](#)
[References](#)
[Tables](#)
[Figures](#)
[◀](#)
[▶](#)
[◀](#)
[▶](#)
[Back](#)
[Close](#)
[Full Screen / Esc](#)
[Print Version](#)
[Interactive Discussion](#)

EGU

NO₂ and HCHO photolysis frequencies

C. Topaloglou et al.

Table 4. Polynomial coefficients for the calculation of $J(\text{HCHO})/J_{\text{pseudo}}=f(E_{325})$ for chemical reaction $\text{HCHO} \rightarrow \text{H} + \text{HCO}$. C_i represents the i degree coefficient.

Solar zenith angle (°)	C_3	C_2	C_1	C_0
15–20	4.283	−4.404	0.193	1.899
20–25	6.552	−7.803	1.885	1.639
25–30	5.825	−6.070	0.949	1.778
30–35	−2.415	0.365	−0.396	1.829
35–40	−7.747	4.491	−1.241	1.876
40–45	−5.227	1.801	−0.226	1.785
45–50	−31.901	16.080	−2.086	1.833
50–55	−92.722	41.708	−4.662	1.889
55–60	−255.563	95.966	−9.138	1.990
60–65	−682.879	202.947	−15.857	2.120
65–70	−1029.41	232.180	−12.427	1.945
70–75	−863.652	166.211	−5.395	1.815
75–80	−5.177.15	626.845	−18.422	1.941
80–85	−10842.9	630.335	−6.472	1.794
85–90	−76310	1924.930	−7.929	1.790

Title Page

Abstract

Introduction

Conclusions

References

Tables

Figures

◀

▶

◀

▶

Back

Close

Full Screen / Esc

Print Version

Interactive Discussion

EGU

NO₂ and HCHO photolysis frequencies

C. Topaloglou et al.

Table 5. Polynomial coefficients for the calculation of $J(\text{HCHO})/J_{\text{pseudo}} = f(E_{325})$ for chemical reaction $\text{HCHO} \rightarrow \text{H}_2 + \text{CO}$. C_i represents the i degree coefficient.

Solar zenith angle (°)	C_3	C_2	C_1	C_0
15–20	5.202	–5.229	0.366	1.892
20–25	6.905	–8.116	1.890	1.649
25–30	6.029	–6.383	1.021	1.776
30–35	–2.016	–0.160	–0.257	1.822
35–40	–7.143	3.741	–1.050	1.868
40–45	–6.598	2.211	–0.234	1.787
45–50	–32.717	16.183	–2.034	1.833
50–55	–100.082	44.429	–4.867	1.895
55–60	–295.819	109.447	–10.297	2.022
60–65	–797.964	233.588	–17.891	2.159
65–70	–1228.350	272.479	–14.237	1.970
70–75	–991.823	186.025	–5.420	1.813
75–80	–5318.360	650.78	–18.192	1.941
80–85	–8042.850	458.765	–1.792	1.775
85–90	–135796	3079.43	–11.693	1.799

[Title Page](#)
[Abstract](#)
[Introduction](#)
[Conclusions](#)
[References](#)
[Tables](#)
[Figures](#)
[◀](#)
[▶](#)
[◀](#)
[▶](#)
[Back](#)
[Close](#)
[Full Screen / Esc](#)
[Print Version](#)
[Interactive Discussion](#)

EGU

**NO₂ and HCHO
photolysis
frequencies**

C. Topaloglou et al.

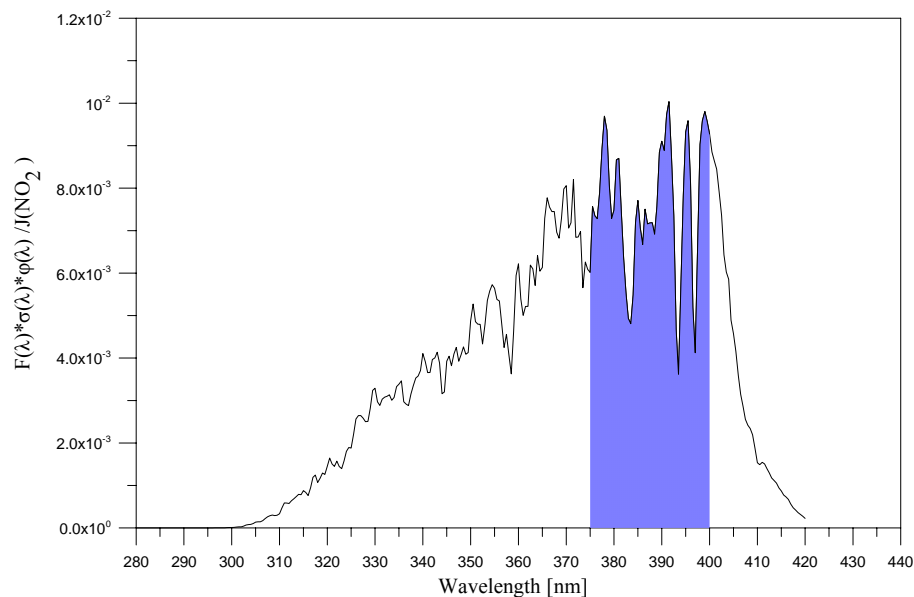


Fig. 1. Relative contribution of each actinic flux wavelength ($F(\lambda) \cdot \sigma(\lambda) \cdot \varphi(\lambda)$) to $J(\text{NO}_2)$ calculation, for $\text{sza}=24^\circ$, on 12 May 2004.

[Title Page](#)[Abstract](#)[Introduction](#)[Conclusions](#)[References](#)[Tables](#)[Figures](#)[◀](#)[▶](#)[◀](#)[▶](#)[Back](#)[Close](#)[Full Screen / Esc](#)[Print Version](#)[Interactive Discussion](#)

EGU

**NO₂ and HCHO
photolysis
frequencies**

C. Topaloglou et al.

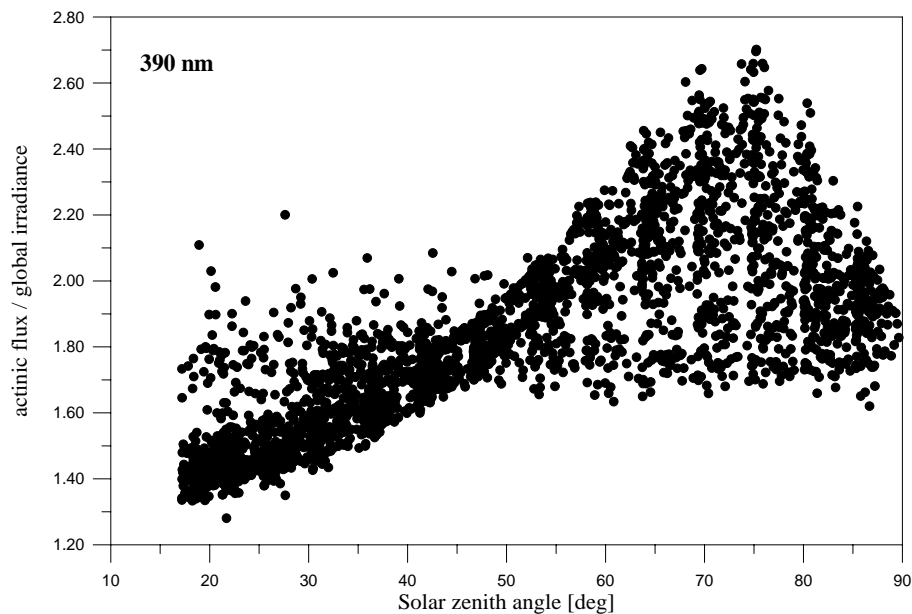


Fig. 2. Ratio of actinic flux/global irradiance at 390 nm as a function of sza. All data are from Bentham measurements in Thessaloniki.

[Title Page](#)[Abstract](#)[Introduction](#)[Conclusions](#)[References](#)[Tables](#)[Figures](#)[◀](#)[▶](#)[◀](#)[▶](#)[Back](#)[Close](#)[Full Screen / Esc](#)[Print Version](#)[Interactive Discussion](#)

EGU

**NO₂ and HCHO
photolysis
frequencies**

C. Topaloglou et al.

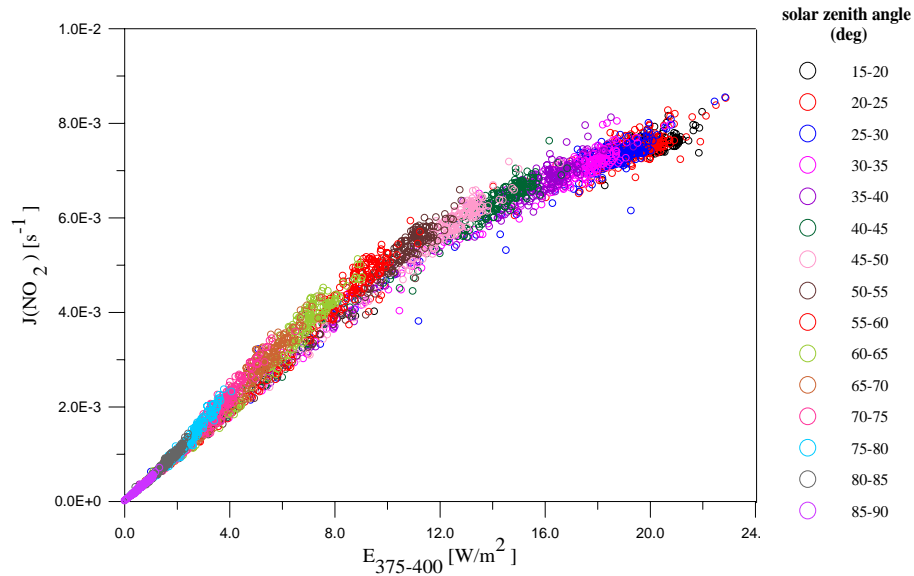


Fig. 3. $J(\text{NO}_2)$ photolysis rates as a function of global irradiance in the region of 375–400 nm.

[Title Page](#)[Abstract](#)[Introduction](#)[Conclusions](#)[References](#)[Tables](#)[Figures](#)[◀](#)[▶](#)[◀](#)[▶](#)[Back](#)[Close](#)[Full Screen / Esc](#)[Print Version](#)[Interactive Discussion](#)

EGU

**NO₂ and HCHO
photolysis
frequencies**

C. Topaloglou et al.

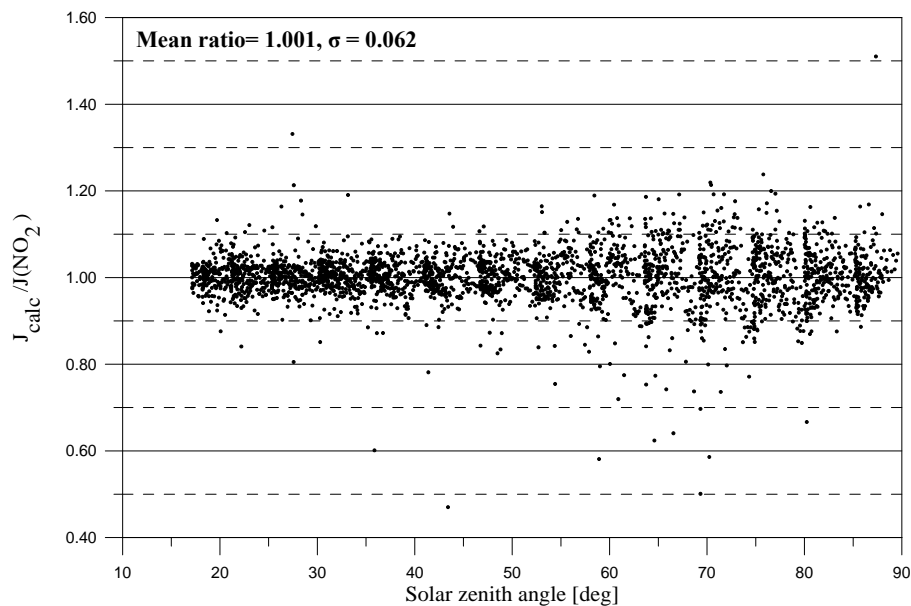


Fig. 4. Ratio of $J(\text{NO}_2)$ calculated by $E_{375-400}$ and polynomials (J_{calc}) over $J(\text{NO}_2)$ estimated by actinic flux versus solar zenith angle. The mean value of the ratio is 1.001 and the standard deviation 0.062.

[Title Page](#)[Abstract](#)[Introduction](#)[Conclusions](#)[References](#)[Tables](#)[Figures](#)[◀](#)[▶](#)[◀](#)[▶](#)[Back](#)[Close](#)[Full Screen / Esc](#)[Print Version](#)[Interactive Discussion](#)

EGU

**NO₂ and HCHO
photolysis
frequencies**

C. Topaloglou et al.

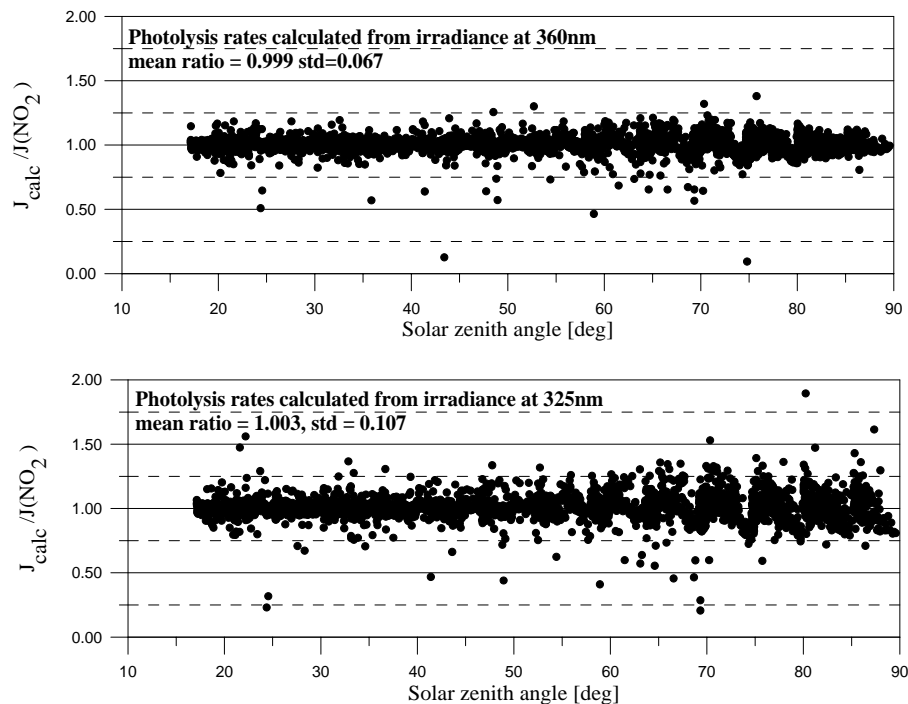


Fig. 5. Ratio of calculated $J(\text{NO}_2)$ from polynomials by the use of global irradiance at 360 nm to $J(\text{NO}_2)$ from actinic flux (upper graph). All data are from the Bentham spectroradiometer. Same ratio for $J(\text{NO}_2)$ calculated from global irradiance at 325 nm (lower graph).

[Title Page](#)[Abstract](#)[Introduction](#)[Conclusions](#)[References](#)[Tables](#)[Figures](#)[◀](#)[▶](#)[◀](#)[▶](#)[Back](#)[Close](#)[Full Screen / Esc](#)[Print Version](#)[Interactive Discussion](#)

EGU

**NO₂ and HCHO
photolysis
frequencies**

C. Topaloglou et al.

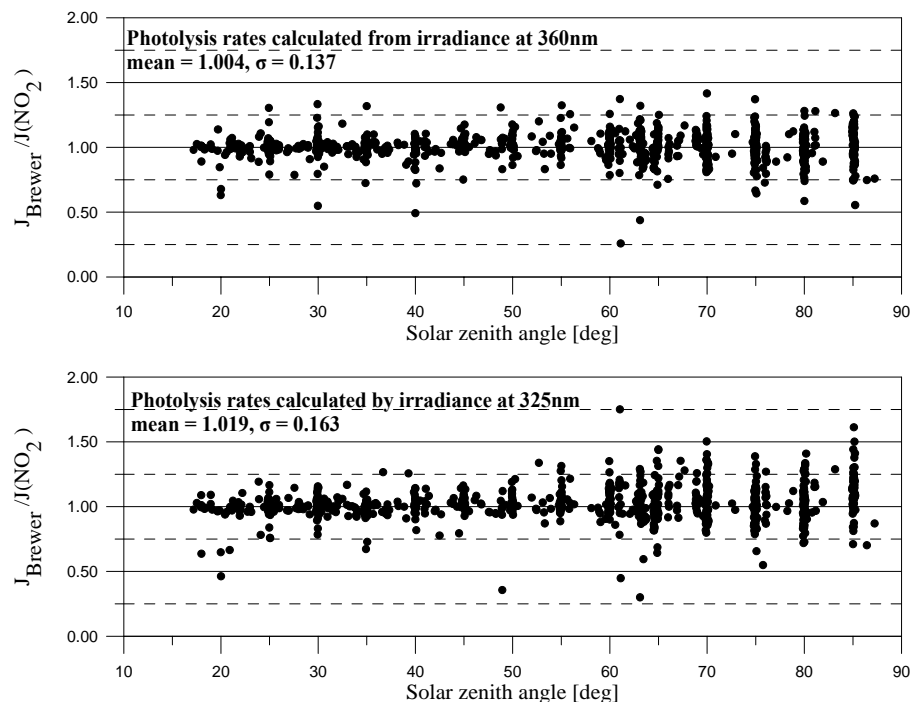


Fig. 6. Ratio of calculated $J(\text{NO}_2)$ from polynomials by the use of global irradiance at 360 nm to $J(\text{NO}_2)$ from actinic flux (upper graph). Same ratio for $J(\text{NO}_2)$ calculated from global irradiance at 325 nm (lower graph).

[Title Page](#)[Abstract](#)[Introduction](#)[Conclusions](#)[References](#)[Tables](#)[Figures](#)[◀](#)[▶](#)[◀](#)[▶](#)[Back](#)[Close](#)[Full Screen / Esc](#)[Print Version](#)[Interactive Discussion](#)

EGU

**NO₂ and HCHO
photolysis
frequencies**

C. Topaloglou et al.

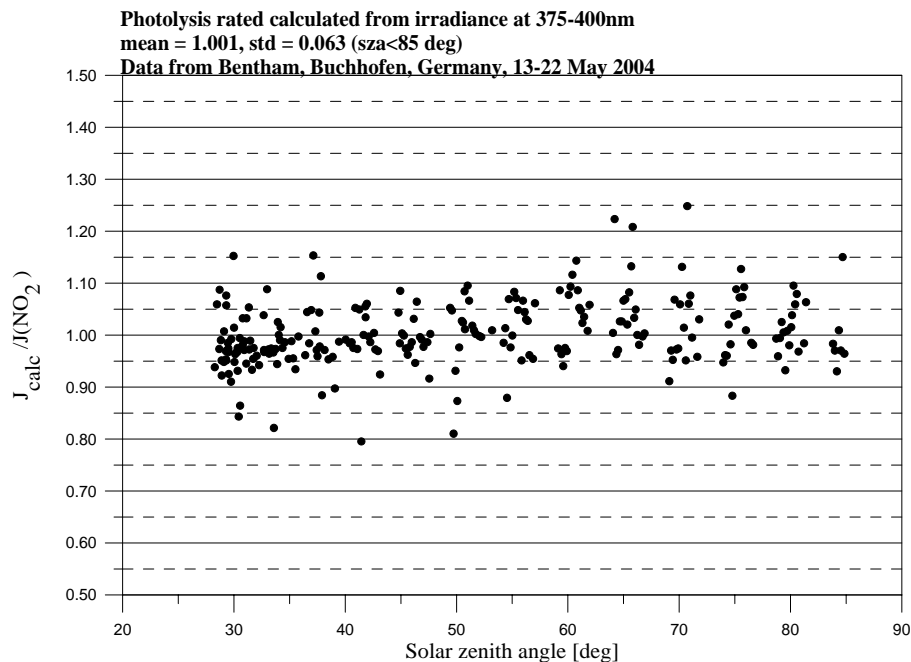


Fig. 7. Ratio of calculated $J(\text{NO}_2)$ from polynomials by the use of $E_{375-400}$ and Thessaloniki polynomials, to $J(\text{NO}_2)$ from actinic flux. All data are provided from a Bentham spectroradiometer from measurements in 13–22 May 2004 in Buchhofen, Germany.

[Title Page](#)[Abstract](#)[Introduction](#)[Conclusions](#)[References](#)[Tables](#)[Figures](#)[◀](#)[▶](#)[◀](#)[▶](#)[Back](#)[Close](#)[Full Screen / Esc](#)[Print Version](#)[Interactive Discussion](#)

EGU

NO₂ and HCHO
photolysis
frequencies

C. Topaloglou et al.

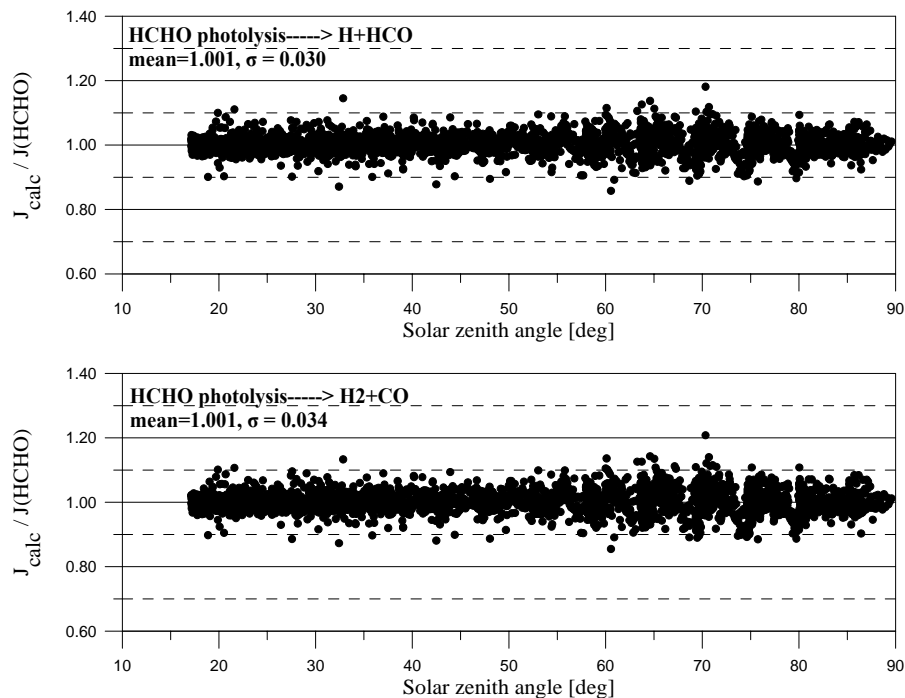


Fig. 8. Ratio of calculated $J(\text{HCHO})$ from polynomials by the use of global irradiance at 325 nm to $J(\text{HCHO})$ from actinic flux for the two chemical reactions of formaldehyde photolysis. All data are provided from the Bentham spectroradiometer.

[Title Page](#)[Abstract](#)[Introduction](#)[Conclusions](#)[References](#)[Tables](#)[Figures](#)[◀](#)[▶](#)[◀](#)[▶](#)[Back](#)[Close](#)[Full Screen / Esc](#)[Print Version](#)[Interactive Discussion](#)

EGU